National Oceanography Centre

Research & Consultancy Report No. 63

A Note on Stommel's Theory of the Tropical Cell

David J. Webb

2018

National Oceanography Centre, Southampton
University of Southampton Waterfront Campus
European Way
Southampton
Hants SO14
3ZH UK

Email: djw@noc.ac.uk

DOCUMENT DATA SHEET

AUTHOR WEBB, DAVID J.	*PUBLICATION DATE* 2018

TITLE
    A note on Stommel's Theory of the Tropical Cell

REFERENCE
    Southampton, UK: National Oceanography Centre, 15pp.
    (National Oceanography Centre Research and Consultancy Report, No. 63)

ABSTRACT

Stommel's theory of wind-drift near the Equator, describing what is now known as the Tropical Cell, is flawed in that it predicts an Equatorial Current and Undercurrent which are much narrower than the observed currents. McCreary's later study with a semi-analytic model showed that the key feature that Stommel had missed was the effect of stratification in the surface layers of the ocean. When stratification is included, it forces the Equatorial upwelling to occur over a much larger range of latitudes. It is also responsible for the changes in sea level and stratification seen close to the Equator. In other respects Stommel's theory appears correct and gives some useful insights into the application of geostrophy near the Equator. This note revisits Stommel's theory, using a slightly different approach, with the aim of providing more details about the solution and also to show how Stommel's simple Ekman layer with geostrophy results in both an Equatorial Current and Equatorial Undercurrent.

KEYWORDS:

ISSUING ORGANISATION   **National Oceanography Centre**
University of Southampton Waterfront Campus
European Way
Southampton SO14 3ZH
UK

PDF available at http://nora.nerc.ac.uk/

Page intentionally left blank

Contents

Page intentionally left blank

A Note on Stommel's Theory of the Tropical Cell

David J. Webb

National Oceanography Centre, Southampton SO14 3ZH, U.K.

Correspondence to: D.J.Webb (djw@noc.ac.uk)

Abstract. Stommel's theory of wind-drift near the Equator, describing what is now known as the Tropical Cell, is flawed in that it predicts an Equatorial Current and Undercurrent which are much narrower than the observed currents. McCreary's later study with a semi-analytic model showed that the key feature that Stommel had missed was the effect of stratification in the surface layers of the ocean. When stratification is included, it forces the Equatorial upwelling to occur over a much larger range of latitudes. It is also responsible for the changes in sea level and stratification seen close to the Equator. In other respects Stommel's theory appears correct and gives some useful insights into the application of geostrophy near the Equator.

This note revisits Stommel's theory, using a slightly different approach, with the aim of providing more details about the solution and also to show how Stommel's simple Ekman layer with geostrophy results in both an Equatorial Current and Equatorial Undercurrent.

1 Introduction

Although it is difficult to observe experimentally, the wind driven surface Ekman layer is known to transport water across the ocean, setting up pressure differences which ultimately drive many of the ocean currents. The net transport in the Ekman layer produced by a given wind stress, depends on the Coriolis parameter and so is a function of latitude, tending to infinity at the Equator. This results seems unrealistic.

In much of the ocean there is also a first order balance between the horizontal pressure gradient within the ocean and the Coriolis term in the equations of motion. This approximation, known as geostrophy, is widely used in ocean studies to derive currents from estimates of the pressure field. The current calculated in this way from a given pressure gradient depends on the Coriolis force and so also tends to infinity at the Equator. Again this seems unrealistic, implying that the underlying theory is breaking down near the Equator.

Stommel (1960) investigated the combined effect of the Ekman transport and geostrophy close to the Equator in an ocean with an unstratified near surface layer and showed that the two effects cancel out. With a steady westward wind stress acting on the ocean, he showed that away from the Equator the solution consists of a surface Ekman layer, with flow away from the Equator, lying above a deeper geostrophic inflow, with a compensating flow towards the Equator. This combined system is now known as the Tropical Cell.

However the solution also generates an Equatorial Current, flowing westwards at the ocean surface and a deeper Equatorial Undercurrent, flowing eastwards. This, a possibly unexpected result, implies that the strength and width of these currents are related to the Ekman spiral in the ocean.

Unfortunately at this point the theory failed. It had one free parameter which was the vertical viscosity. If a physically realistic value was chosen, the speed of the Equatorial Current and Undercurrent were reasonable, with value around $1.5 \, \mathrm{m \, s^{-1}}$, but the width was only a fraction of a degree, compared to the observed width of one to two degrees. If the viscosity was increased, the a reasonable width can be obtained but the speeds drop to $0.15 \, \mathrm{m \, s^{-1}}$. Thus the theory appeared to contain a major flaw.

The source of the problem was eventually explained by McCreary (1981), who showed that it was necessary to introduce stratification. He developed a semi-analytic model of the Equatorial system and found that upwelling near the Equator was limited by the rate at which heat could diffuse downwards. One result of this was to increase the range of latitudes over which upwelling occurs. The Ekman transport also reduces sea level near the Equator and generates a compensating uplift of the density surfaces below. This increases the vertical temperature gradient, which together with the in-

creased latitudinal spread, results in the required downward diffusion of heat.

Returning to the Stommel (1960) paper, the study is still of interest because of the way it shows that both Ekman theory and geostrophy remain valid as the Equator is approached. Unfortunately, and partly because he already knew its limitations, Stommel's paper only includes one schematic figure of the solution and it does not really try and explain how the Ekman spiral and geostrophy combine to give the Equatorial Current and Undercurrent as the Equator is approached.

The present note returns to the Stommel problem and attempts to provide better illustrations of the solution and to investigate the limit as the Equator is approached. Section two of the paper is concerned with the analytic model, using a slightly different approach to the one used by in Stommel (1960). Full details of the analytic solution are included in the Appendices and these also include the limiting solutions as the distance to the Equator becomes very large or very small.

The main results are presented in section three and used in section four to investigate the behaviour of the Ekman spiral near the Equator. Finally section five briefly discusses the results.

2   The Analytic Model

Oceanographic sections across the Equator, show that at low latitudes below the surface mixed layer there is a region of strong stratification usually associated with the Equatorial Undercurrent. The layer, which extends a few degrees on either side of the Equator, is so strongly stratified that vertical motions through the layer are likely to be small.

However the infinity in the Ekman transport that occurs as one approaches the Equator, means that at low latitudes the transport is rapidly changing. Under normal oceanographic conditions this would imply a large amount of Ekman suction and vertical velocities at the base of the Ekman layer which tend to infinity as the Equator is approached.

However, because of the observed strongly stratified layer, this cannot occur. Stommel therefor made the simplification that the near surface ocean as a simple mixed layer of uniform density. He also assumed that the layer thickness was constant and there there was no flow through its bottom boundary.

The Equatorial Current has a maximum velocity in the region of high density gradient, i.e. at the bottom of the model mixed layer. If the vertical viscosity is constant then a maximum in the velocity implies a zero vertical stress, at least in the zonal direction. On this basis the model assumes zero stress, in both directions, at the base of the mixed layer.

At the surface the model assumes a constant zonal wind stress to the west. Munk's circulation theory showed that currents at the Equator can be generated by a non-zero wind stress curl. Such solutions bypass the infinity problem at the

Equator because it is always possible to construct a stress field with the same curl but with zero stress at the Equator. The case considered here, where the wind stress is constant, would produce no flow in the Munk model, but it would be possible later to add a Munk type solution to the present results and so represent the effect of a varying wind stress field.

Stommel's model also assumes that the integrated zonal pressure gradient balances the wind stress. The justification for doing this is based on observational evidence (i.e. Bryden and Brady (1985)) and model analysis.

Finally the model assumes that the zonal pressure gradient, like the wind stress, is independent of latitude. In the surface layer there can be some density effects but the pressure gradients are generated primarily by changes in the height of the sea surface. Experience with a high-resolution version of the NEMO model shows that in the central Pacific the time averaged zonal gradient in SSH, which increases to the west, is roughly constant in the latitudes spanning the Equator.

Of all these assumptions the key factor is that the meridional Ekman transport and the meridional geostrophic transport balance within the layer being studied. When this is true the infinities disappear and a reasonable solution can be obtained even very close to the Equator.

2.1   The Model Equations

If we assume that the ocean is incompressible and that, in the vertical, it is in hydrostatic balance, the equations describing the system are,

$$\rho(\frac{\partial u}{\partial t} + u\frac{\partial u}{\partial x} + v\frac{\partial u}{\partial y} + w\frac{\partial u}{\partial z} - fv) =$$
$$\frac{\partial p}{\partial x} + \kappa\frac{\partial^2 u}{\partial z^2} + A_h(\frac{\partial^2 u}{\partial x^2} + \frac{\partial^2 u}{\partial y^2}), \quad (1)$$

$$\rho(\frac{\partial v}{\partial t} + u\frac{\partial v}{\partial x} + v\frac{\partial v}{\partial y} + w\frac{\partial v}{\partial z} + fu) =$$
$$\frac{\partial p}{\partial y} + \kappa\frac{\partial^2 v}{\partial z^2} + A_h(\frac{\partial^2 v}{\partial x^2} + \frac{\partial^2 v}{\partial y^2}), \quad (2)$$

$$0 = \frac{\partial p}{\partial z} + \rho g, \quad (3)$$

$$\frac{\partial u}{\partial x} + \frac{\partial v}{\partial y} + \frac{\partial w}{\partial z} = 0. \quad (4)$$

where u, v and w are the components of velocity in the eastwards, northwards and upwards directions corresponding to co-ordinates x, y and z. ρ is density, t is time and p is pressure. κ is the vertical and A_h the horizontal viscosity coefficient, both assumed constant. g is gravity.

The Coriolis parameter f is defined as,

$$f = 2\Omega\sin(\theta). \quad (5)$$

where Ω is the Earth's rotation rate and θ the latitude.

Stommel looked for the steady state solution for a well mixed surface layer of thickness H and constant density ρ_0.

Velocities are assumed to be small so the advection terms can be neglected. The horizontal viscosity terms are also assumed to be small enough to be neglected. Equation 3 can then be solved to give,

$$p(x, y, z) = p_0(x, y) + \rho_0 g z, \qquad (6)$$

and Eqns. 1 and 2 become,

$$
\begin{aligned}
-\rho_0 f v &= \frac{\partial p_0}{\partial x} + \kappa \frac{\partial^2 u}{\partial z^2}, \\
\rho_0 f u &= \frac{\partial p_0}{\partial y} + \kappa \frac{\partial^2 v}{\partial z^2}.
\end{aligned}
\qquad (7)
$$

For boundary conditions, Stommel assumed that at the top of the layer, the ocean surface, there was a wind stress τ_x acting in the x direction only and that the wind stress exactly balanced the vertical integral of the horizontal pressure gradient. He also assumed that at the bottom of the layer there was zero stress. The equations relating pressure and wind stress are then

$$
\begin{aligned}
\int_{-H}^{0} dz \frac{\partial p_0}{\partial x} &= \tau_x, \\
\int_{-H}^{0} dz \frac{\partial p_0}{\partial y} &= 0,
\end{aligned}
\qquad (8)
$$

and the surface and bottom boundary conditions are,

$$
\begin{aligned}
\kappa \frac{\partial u}{\partial z} &= \tau_x \quad and \quad \kappa \frac{\partial v}{\partial z} = 0 \quad at \quad z = 0, \\
\kappa \frac{\partial u}{\partial z} &= 0 \quad and \quad \kappa \frac{\partial v}{\partial z} = 0 \quad at \quad z = -H.
\end{aligned}
\qquad (9)
$$

2.2 Method of Solution

Stommel solved the problem by splitting the two horizontal components of velocity u and v into Ekman and geostrophic components,

$$
\begin{aligned}
u &= u_e + u_g, \\
v &= v_e + v_g.
\end{aligned}
\qquad (10)
$$

The geostrophic components balance the pressure gradient terms in Eqn. 7.

$$
\begin{aligned}
-\rho_0 f v_g &= \frac{\partial p_0}{\partial x}, \\
\rho_0 f u_g &= \frac{\partial p_0}{\partial y}.
\end{aligned}
\qquad (11)
$$

Integrating these equations over depth and using Eqn. 8 gives the solutions,

$$
\begin{aligned}
u_g &= 0 \\
v_g &= \frac{\tau_x}{\rho_0 f H}.
\end{aligned}
\qquad (12)
$$

As the Equator is approached v_g has a singularity proportional to $1/f$.

2.3 The Ekman Components

The Ekman components balance the vertical viscosity terms in Eqn. 7,

$$
\begin{aligned}
-\rho_0 f v_e &= \kappa \frac{\partial^2 u_e}{\partial z^2}, \\
\rho_0 f u_e &= \kappa \frac{\partial^2 v_e}{\partial z^2}.
\end{aligned}
\qquad (13)
$$

with boundary conditions,

$$
\begin{aligned}
\kappa \frac{\partial u_e}{\partial z} &= \tau_x \quad and \quad \kappa \frac{\partial v_e}{\partial z} = 0 \quad at \quad z = 0, \\
\kappa \frac{\partial u_e}{\partial z} &= 0 \quad and \quad \kappa \frac{\partial v_e}{\partial z} = 0 \quad at \quad z = -H.
\end{aligned}
\qquad (14)
$$

Details of the method used to solve these equations is given in Appendix I. The solutions are,

$$
\begin{aligned}
u_e(y, z) &= u_1 e^{\alpha(1+i)z/H} + u_3 e^{-\alpha(1+i)(z/H)} + c.c., \\
v_e(y, z) &= -i \left(u_1 e^{\alpha(1+i)z/H} + u_3 e^{-\alpha(1+i)(z/H)} \right) + c.c..
\end{aligned}
\qquad (15)
$$

where "$c.c.$" represents complex conjugate and,

$$
\alpha = \left(\frac{\rho_0 f H^2}{2\kappa} \right)^{1/2}. \qquad (16)
$$

$$
\begin{aligned}
u_1 &= \left(\frac{\tau_x H}{\kappa} \right) \frac{1}{2\alpha(1+i)(1 - e^{-2\alpha(1+i)})}, \\
u_3 &= \left(\frac{\tau_x H}{\kappa} \right) \frac{1}{2\alpha(1+i)(1 - e^{2\alpha(1+i)})}.
\end{aligned}
\qquad (17)
$$

There are two limits of interest. Far from the Equator, α is large and as a result the ratio of u_3 to u_1 tends to zero. In this limit the two components of velocity become,

$$
\begin{aligned}
u_e(z) &\approx \left(\frac{\tau_x H}{\kappa} \right) \frac{1}{\sqrt{2}\alpha} e^{\alpha z} sin(\alpha z - \pi/4), \\
v_e(z) &\approx \left(\frac{\tau_x H}{\kappa} \right) \frac{1}{\sqrt{2}\alpha} e^{\alpha z} cos(\alpha z - \pi/4).
\end{aligned}
\qquad (18)
$$

corresponding to a normal Ekman spiral.

Near the Equator α is small. Appendix A shows that in this limit the functions have the form,

$$
u_e(z) \approx \left(\frac{\tau_x H}{\kappa} \right) \frac{1}{6} (2 + 6z + 3z^2) + O(\alpha^4),
$$

$$
v_e(z) \approx -\left(\frac{\tau_x H}{\kappa} \right) \left[\frac{1}{2\alpha^2} + \alpha^2 \frac{-8 + 60z^2 + 60z^3 + 15z^4}{180} \right] + O(\alpha^6).
$$

Substituting for α,

$$
v_e(z) \approx -\frac{\tau_x}{\rho f H} \quad + \quad O(\alpha^2). \qquad (19)
$$

Thus near the Equator u_e is well behaved but v_e has a singularity, proportional to $1/f$. This exactly balances the singularity in the geostrophic velocity v_g (Eqn. 12).
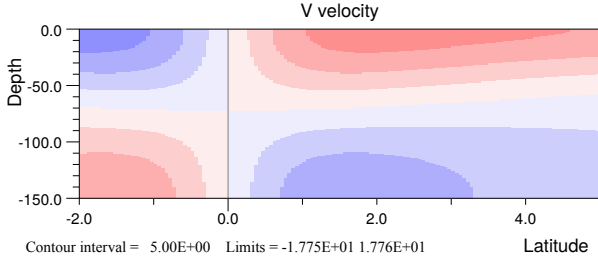
Figure 1. Northward component of velocity. Red (blue) indicates northward (southward) velocity. Contours at intervals of $5\ \mathrm{cm\,s^{-1}}$.

Figure 3. Zonal velocity field. Red (blue) indicates eastward (westward) flow. Contours at intervals of $5\ \mathrm{cm\,s^{-1}}$.
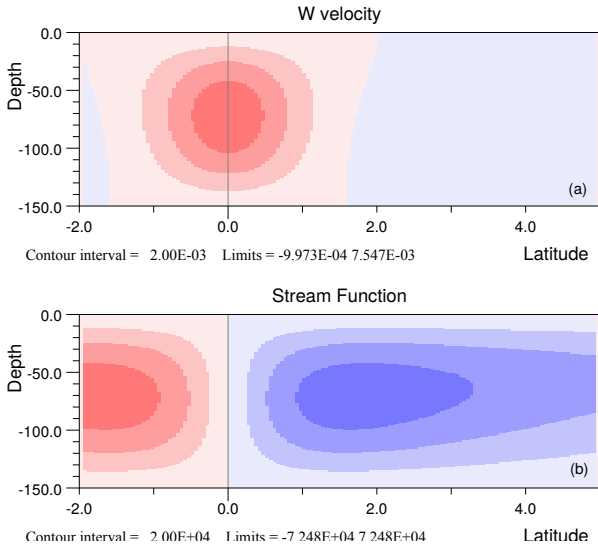

Figure 2. (a) The vertical component of velocity. Red (blue) indicates upward (downward) motion. Contours at intervals of 2×10^{-3} $\mathrm{cm\,s^{-1}}$. (b) Meridional stream function. Red (Blue) indicates anti-clockwise (clockwise) flow. Contours at intervals of $2 \times 10^{4}\ \mathrm{cm^{2}s^{-1}}$

3   The Solution as a Function of Latitude

Figures 1 to 3 show the solution for an east-west wind stress τ_x of -0.1 Pa (-1 $\mathrm{dyne\,cm^{-2}}$), i.e. for a wind blowing towards the west[1]. The thickness of the ocean surface layer is 150 m, the density of water is assumed to be 1000 $\mathrm{kg\,m^{-3}}$ and the vertical viscosity coefficient is 10 Pl (100 $\mathrm{gm\,cm^{-1}\,s^{-1}}$). In terms of Appendix I, the scaling factor for the non-dimensional velocity $(\tau H/\kappa)$ is then 1.5 $\mathrm{m\,s^{-1}}$ and the latitude corresponding to an α value of 2 is 1.05° north or south. As discussed in the Appendix, this is a measure of the width of the Equatorial Current and Undercurrent.

As the flow is symmetric about the Equator, each figure shows only part of the southern hemisphere solution. At the

[1]In these figures, limits refer to minimum and maximum values at the centre of plotted cells, not absolute limits.
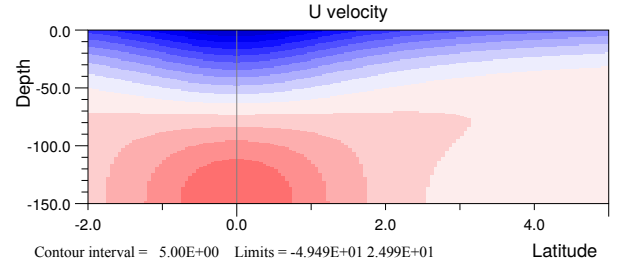
surface, the Ekman layer transports surface water away from the Equator, the thickness of the layer becoming smaller as latitude increases. The velocity is zero at the Equator itself and increases rapidly to near 2°N, after which it decays. At depth the flow is towards the Equator, again with a maximum velocity near 2°N, and zero velocity at the Equator itself.

Figure 2 shows that the main area of upwelling occurs within one degree of the equator. This is compensated by downwelling at higher latitudes, the maxima occuring near 2° north and south. The resulting circulation, equivalent to the topical overturning cell, shows up clearly in the stream function figure. The transport in the cell is $7.3 \times 10^4\ \mathrm{cm^2s^{-1}}$, equivalent to 0.81 Sverdrups per degree of longitude.

The eastward component of velocity is shown in Fig. 3. Away from the Equator, the velocities behave as expected from an Ekman spiral, with surface velocities in the direction of the wind, a reversed flow below and a further change in direction at depth.

As the Equator is approached the surface flow becomes much stronger in the region where the north-south velocity tends to zero. It may thus be identified as the representation of the Equatorial Current. Below there is a strong reverse current at the right depths for the Equatorial Undercurrent.

Overall the results show that although the Ekman and geostrophic solution each generate unphysical singularities as the Equator is approached, the combined solution is well behaved, although weaker than observed in reality. The full solution not only generates the Ekman outflow and geostrophic inflow at high latitudes, but the combined solution also generates the tropical overturning cells and both the Equatorial Current and Undercurrent.

3.1   Varying Viscosity and Layer depth

If $\Psi(x,z)$ and is the stream function in real space and $\psi(\alpha, z')$ the stream function in the non-dimensional space used in Appendix A, then from Eqn. A20,

$$\Psi(x,z) = \left(\frac{\tau H^2}{\kappa}\right)\psi(\alpha, z'). \tag{20}$$

The strength of the Tropical Cell is thus proportional to the square of the layer depth and to the inverse of the vertical viscosity.

Near the Equator, the Coriolis term is an approximately linear function of latitude. Thus substituting βx for f in Eqn. 16 and rearranging,

$$x = \left(\frac{2\kappa}{\rho_0 \beta H^2}\right)\alpha^2. \tag{21}$$

Thus the contribution of layer depth and vertical viscosity to the latitudinal scale of the Tropical Cell, is the inverse of their contribution to its strength.

4 The Ekman Spiral near the Equator

In order to understand the reason for the solution's behaviour near the Equator, Fig. 4 plots the horizontal components of velocity as a function of depth for values of α (Eqn. 17) between 0.5 and 5.0. The variable α is proportional to $f^{1/2}$, so low values of α correspond to latitudes near the Equator.

For this figure the normal axis directions have been rotated by ninety degrees so that the horizontal 'x' axis corresponds to north and the vertical 'y' axis to west. The figure also shows non-dimensional velocities, which should be multiplied by $(\tau H/\kappa)$ to convert to dimensional values.

Far from the equator, where α is large, the locii take the form of a traditional Ekman spiral, with the surface velocity at 45 degrees to the surface wind stress. As depth increases the velocity vector rotates clockwise, in the northern hemisphere, and its magnitude decreases exponentially with depth.

As α is reduced, the velocities increases by an amount roughly proportional to α^{-2} (i.e. f^{-1}) but as α drops below a value of 2 there are two significant changes. First the surface velocity in the direction of the wind increases more slowly, eventually reaching a value of 1/3 in the limit of infinite α (Eqn. A15). Secondly the Ekman spiral starts to unwind, the velocity at depth no longer tending to zero. Instead the velocity in the direction of the wind becomes negative, eventually reaching a value of -1/6 in the limit of infinite α.

The overall result is that, as the Equator is approached, the Ekman velocities increase and a form of Ekman spiral continues to exist, but in the limit, the shear between the top and bottom of the surface layer becomes aligned with the wind.

4.0.1 Adding the Geostrophic Term

The effect of adding the geostrophic term is shown in Fig 5. At small values of α the combined solution has the form of an Ekman spiral but with an offset corresponding to the geostrophic inflow.

As α is reduced the spiral unwinds and it is during this process, at values near α equal to 2, that the surface and bottom velocities at right angles to the wind are greatest. As α is
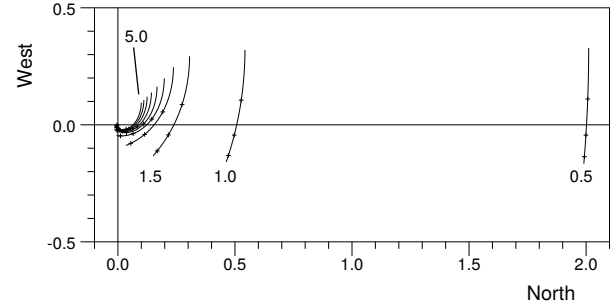

Figure 4. The non-dimensional velocities plotted as set of Ekman spirals (i.e. (u,v) plotted as a function of depth) for values of α between 0.5 and 5.0, at intervals of 0.5. The axes have been rotated clockwise so that the wind stress vector runs vertically. The crosses correspond to non-dimensional depths of 0.25, 0.5 and 0.75, the shallowest depths having a positive velocity both westwards and northwards.
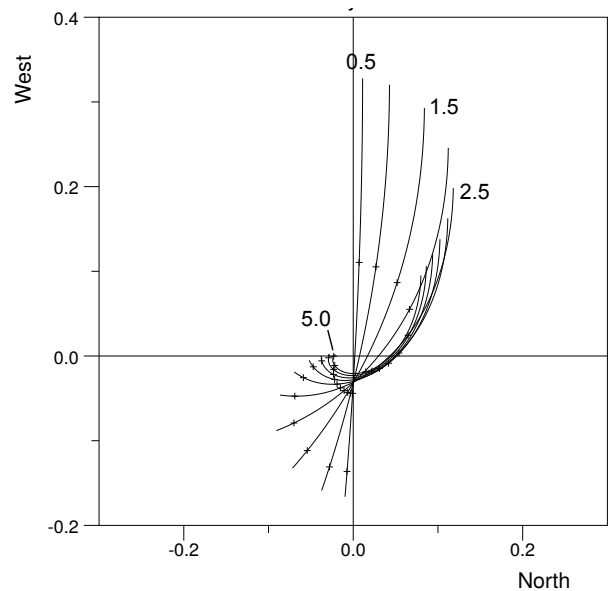

Figure 5. As Fig. 4, except that the velocities are plotted after subtracting the contribution of the geostrophic current $(1/2\alpha^2)$.

reduced further the locii become more linear, the velocity at right angles to the wind tending to zero in the limit of infinite α.

The result implies that it is the unwinding of the Ekman spiral which, as the Equator is approached, gives the smooth transition to the Equatorial Current and Undercurrent.

5 Conclusions

Although Ekman theory and geostrophic theory both generate infinite currents at the Equator, when they are combined in an model of an unstratified surface layer, the resulting flow field satisfactorily reproduces many of the near surface features of the equatorial ocean. These include the surface Ekman layer transport away from the Equator, the deeper geostrophic inflow, the resulting tropical cell, and both the Equatorial Current and the Equatorial Undercurrent.

In reality, as discussed by McCreary (1981), stratification in the surface layer is important. However although this affects the width of the Equatorial Current and Undercurrent, this unwinding of the Ekman spiral as the Equator is approached is still likely to be valid.

Appendix A: Solution of the Analytic Model

Non-dimensional the variables by making the substitutions,

$$
\begin{aligned}
z &= z'H, \\
u_e &= u'_e(\tau H/\kappa), \\
v_e &= v'_e(\tau H/\kappa).
\end{aligned}
\tag{A1}
$$

Eqns. 13 then become,

$$
\begin{aligned}
-\rho f v'_e &= \frac{\kappa}{H^2}\frac{\partial^2 u'_e}{\partial z'^2}, \\
\rho f u'_e &= \frac{\kappa}{H^2}\frac{\partial^2 v'_e}{\partial z'^2},
\end{aligned}
\tag{A2}
$$

with boundary conditions,

$$
\begin{aligned}
\frac{\partial u'_e}{\partial z'} &= 1 \quad and \quad \frac{\partial v'_e}{\partial z'} = 0 \quad at \quad z' = 0, \\
\frac{\partial u'_e}{\partial z'} &= 0 \quad and \quad \frac{\partial v'_e}{\partial z'} = 0 \quad at \quad z' = -1.
\end{aligned}
\tag{A3}
$$

In the rest of this section, the primes will be dropped. We look for solutions of the form,

$$
u_e = u\exp(kz), \qquad v_e = v\exp(kz).
\tag{A4}
$$

From Eqn.A2,

$$
\begin{aligned}
-\rho f v\, e^{kz} &= \frac{\kappa}{H^2}k^2 u\, e^{kz}, \\
\rho f u\, e^{kz} &= \frac{\kappa}{H^2}k^2 v\, e^{kz}.
\end{aligned}
\tag{A5}
$$

Eliminating v,

$$
(\rho f)^2 u = -\left(\frac{\kappa}{H^2}\right)^2 k^4 u.
\tag{A6}
$$

So,

$$
k^4 = -\left(\frac{\rho f H^2}{\kappa}\right)^2.
\tag{A7}
$$

If,

$$
\alpha = \left(\frac{\rho f H^2}{2\kappa}\right)^{1/2}
\tag{A8}
$$

then

$$
k = \alpha(\pm 1 \pm i).
\tag{A9}
$$

The general solution is thus,

$$
\begin{aligned}
u_e =&\, u_1 e^{\alpha(1+i)z} + u_2 e^{\alpha(1-i)z} \\
&+ u_3 e^{-\alpha(1+i)z} + u_4 e^{-\alpha(1-i)z},
\end{aligned}
$$

$$
\begin{aligned}
v_e =&\, \frac{-1}{2\alpha^2}[u_1\alpha^2(1+i)^2 e^{\alpha(1+i)z} + u_2\alpha^2(1-i)^2 e^{\alpha(1-i)z} \\
&+ u_3\alpha^2(1+i)^2 e^{-\alpha(1+i)z} + u_4\alpha^2(1-i)^2 e^{-\alpha(1-i)z}], \\
=&-i\ [u_1 e^{\alpha(1+i)z} - u_2 e^{\alpha(1-i)z} \\
&+ u_3 e^{-\alpha(1+i)z} - u_4 e^{-\alpha(1-i)z}].
\end{aligned}
$$

and the vertical derivatives become,

$$
\begin{aligned}
\frac{\partial u_e}{\partial z} =&\ u_1\alpha(1+i)e^{\alpha(1+i)z} + u_2\alpha(1-i)e^{\alpha(1-i)z} \\
&-u_3\alpha(1+i)e^{-\alpha(1+i)z} - u_4\alpha(1-i)e^{-\alpha(1-i)z}, \\
\frac{\partial v_e}{\partial z} =&\ -i\ [u_1\alpha(1+i)e^{\alpha(1+i)z} - u_2\alpha(1-i)e^{\alpha(1-i)z} \\
&-u_3\alpha(1+i)e^{-\alpha(1+i)z} + u_4\alpha(1-i)e^{-\alpha(1-i)z}].
\end{aligned}
$$

The boundary conditions at the surface give,

$$
\begin{aligned}
1 &= u_1\alpha(1+i) + u_2\alpha(1-i) - u_3\alpha(1+i) - u_4\alpha(1-i), \\
0 &= u_1\alpha(1+i) - u_2\alpha(1-i) - u_3\alpha(1+i) + u_4\alpha(1-i).
\end{aligned}
$$

and at the bottom boundary, where z equals -1,

$$
\begin{aligned}
0 &= u_1\alpha(1+i)e^{-\alpha(1+i)} + u_2\alpha(1-i)e^{-\alpha(1-i)} \\
&\quad -u_3\alpha(1+i)e^{\alpha(1+i)} - u_4\alpha(1-i)e^{\alpha(1-i)}, \\
0 &= u_1\alpha(1+i)e^{-\alpha(1+i)} - u_2\alpha(1-i)e^{-\alpha(1-i)} \\
&\quad -u_3\alpha(1+i)e^{\alpha(1+i)} + u_4\alpha(1-i)e^{\alpha(1-i)}.
\end{aligned}
$$

Combining these equations,

$$
\begin{aligned}
1 &= 2u_1\alpha(1+i) - 2\alpha u_3(1+i), \\
0 &= 2u_1(1+i)e^{-\alpha(1+i)} - 2u_3(1+i)e^{\alpha(1+i)}.
\end{aligned}
\tag{A10}
$$

Thus,

$$
u_3 = u_1 e^{-2\alpha(1+i)},
\tag{A11}
$$

and,

$$
\begin{aligned}
u_1 &= \frac{1}{2\alpha(1+i)(1-e^{-2\alpha(1+i)})}, \\
u_3 &= \frac{-1}{2\alpha(1+i)(1-e^{2\alpha(1+i)})}.
\end{aligned}
\tag{A12}
$$

Repeating the process for u_2 and u_4, one finds that these are the complex conjugates of u_1 and u_3. In non-dimensional form the geostrophic term (Eqn 1) is,

$$v_g = \frac{1}{2\alpha^2}. \tag{A13}$$

Combining the Ekman and geostrophic components, the full solution is,

$$
\begin{aligned}
u(z) &= [u_1 e^{\alpha(1+i)z} + u_3 e^{-\alpha(1+i)z}] + c.c., \\
v(z) &= -i[\,u_1 e^{\alpha(1+i)z} + u_3 e^{-\alpha(1+i)z)}] + c.c. \\
&\qquad\qquad +1/(2\alpha^2). \tag{A14}
\end{aligned}
$$

where $c.c.$ represents the complex conjugate terms.

A1   Behaviour at Small and Large α

The parameter α is proportional to $f^{1/2}$, so it tends to zero as the Equator is approached. An expansion of the Ekman part of Eqns. A14 in a Taylor series about this limit was carried out using an algebraic manipulator (Maxima). When α is small, the Ekman components become,

$$u_e(z) \approx \frac{1}{6}(2 + 6z + 3z^2) + O(\alpha^4), \tag{A15}$$

$$v_e(z) \approx -\frac{1}{2\alpha^2} + \alpha^2 \frac{-8 + 60z^2 + 60z^3 + 15z^4}{180}$$
$$+ O(\alpha^6). \tag{A16}$$

The first equation shows that at the Equator, $u_e(z)$ is a well defined function of z with no singularity. As α increases away from the Equator, the correction term is proportional to f^2, showing that $u_e(z)$ is a parabolic function of f and thus, to first order, a parabolic function of latitude.

The second equation shows that the leading term in $v_e(z)$ has a singularity at the Equator which is proportional to $1/f$ but independent of depth. If this is subtracted out, the function is zero at the Equator and initially increases linearly with f away from the Equator.

Far from the Equator, where α is large, the exponential functions in Eqns. A12 tend to zero. As a result, in this limit,

$$
\begin{aligned}
u_1 &\approx \frac{1}{2\alpha(1+i)}, \\
u_3 &\approx 0. \tag{A17}
\end{aligned}
$$

After some algebra the solutions are,

$$u_e(z) \approx \frac{1}{\sqrt{2}\alpha} e^{\alpha z} \sin(\alpha z - \pi/4), \tag{A18}$$

$$v_e(z) \approx \frac{1}{\sqrt{2}\alpha} e^{\alpha z} \cos(\alpha z - \pi/4). \tag{A19}$$

This form corresponds to a standard Ekman spiral, the vector (u,v) rotating and decaying with depth.

	Value of α	Value of $u(z)$
$u(0,0)$	0.0000	1/3
$u(0,-1)$	0.0000	-1/6
Minimum $\partial u(\alpha,0)/\partial(\alpha)$	1.9859	0.2522
Maximum $\partial u(\alpha,-1)/\partial(\alpha)$	1.9318	-0.0946
$u(0,-1)=0$	3.9266	0.0000
		$v(\alpha,z)$
$v(0,0)$	0.0000	0.0000
$v(0,-1)$	0.0000	0.0000
Maximum of $v''(\alpha,0)$	2.4092	0.1184
Minimum of $v''(\alpha,-1)$	2.1323	-0.0917

Table A1. Values of α and the two components of velocity, $u(\alpha,z)$ and $v(\alpha,z)$, at key locations on the surface (z=0) and at maximum depth (z=-1).

A2   Behaviour at the Surface and Bottom of the Layer

The functions $u(z)$ and $v(z)$ (Eqns. A14) are plotted in Fig.A1 for the surface (z=0) and for the bottom of the layer (z=-1). The values of α at key points are given in table A1. The maximum and minimum values of v and the greatest gradients of u occur in the region of α equal to 2. The first zero crossing of $u(-1)$ occurs in the region of α equal to 4.

Far from the Equator, where α is large, the solutions are consistent with the normal behaviour of an Ekman spiral. The velocity at the surface is at 45°to the wind and the velocity tends to zero at depth.

Near the Equator, where α is small, the meridional component v tends to zero. At the Equator itself, the zonal component u, is in the direction of the wind at the surface and reverses at depth, the maximum speed at the surface (1/3) being twice that of undercurrent at the bottom of the layer ($-1/3$). In between the current is zero at depth z_{u0}, where,

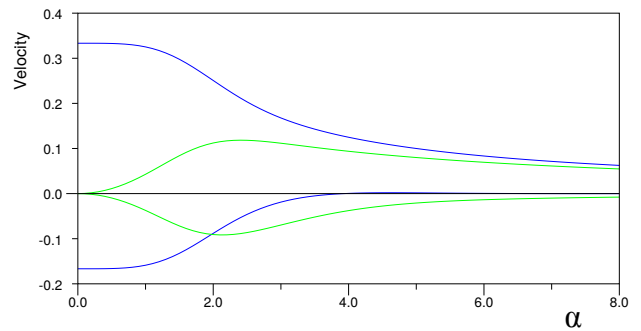$$z_{u0} = -1 + (1/3)^{1/2} \approx -0.4226.$$

Figure A1. Non-dimensional components of velocities u and v (Eqn. A14), on the surface (z=0) and at maximum depth (z=-1), plotted as function of α.
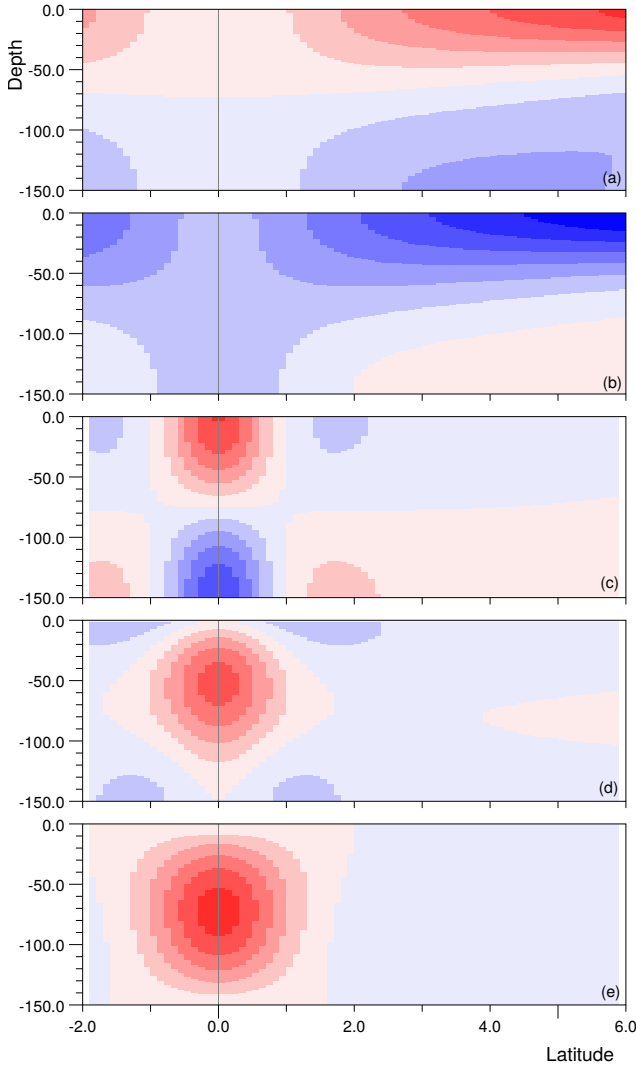
Figure A2. Force eastwards per unit volume (Nm^{-3}) due to (a) vertical component of Coriolis vector (contour interval 4×10^{-4}), (b) vertical viscosity (4×10^{-4}), (c) horizontal viscosity (10^{-6}), (d) advection (10^{-4}), (e) horizontal component of Coriolis vector (2×10^{-6}).

A3   The Stream Function

The non-dimensional meridional stream function Ψ is defined by the equation,

$$\Psi(\alpha, z) = \int\limits_{z}^{0} dz' \ v(\alpha, z'). \tag{A20}$$

Substituting for v from Eqn. A14 and integrating over z,

$$\Psi(\alpha, z) = \frac{-1}{4\alpha^2} \left(\frac{1 - e^{\alpha(1+i)z}}{1 - e^{-2\alpha(1+i)}} + \frac{1 - e^{-\alpha(1+i)z}}{1 - e^{2\alpha(1+i)}} \right)$$
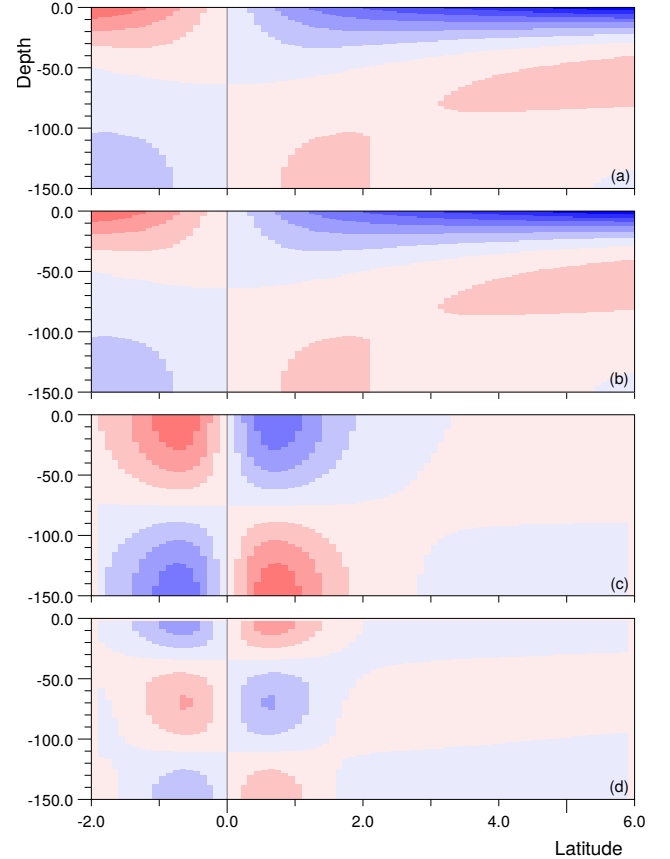$$+ \ c.c. + \frac{z}{2\alpha^2}. \tag{A21}$$

Figure A3. Force northwards per unit volume (Nm^{-3}) due to (a) vertical component of Coriolis vector (contour interval 4×10^{-4}), (b) vertical viscosity 4×10^{-4}, (c) horizontal viscosity 10^{-6}, (d) advection 5×10^{-5}.

The maximum value, where Ψ equals 0.03221 occurs at α equal to 2.2262 and z equal to -0.4630.

A4   Other Terms in the Equation

For the case discussed above, the constant zonal pressure gradient term $(\partial p/\partial x)$ in Eqn. 1 has a value of $3.3 \ 10^{-4} \mathrm{Nm}^{-3}$. Figure A2 shows the size of the other terms in the zonal equation, after the Coriolis and advection terms have been transferred to the right hand side. All positive values thus correspond to forces towards the east.

Thus the surface flow away from the Equator generates, through the Coriolis term $(\rho f v)$, a force to the east which is balanced partly by the vertical viscosity term $(\kappa \partial^2 u/\partial z^2)$ and the remainder by the constant zonal pressure gradient. At the Equator the Coriolis term is zero so vertical viscosity exactly balances the zonal pressure gradient.

The figure also shows the size of terms neglected in the analytic model described above. Horizontal viscosity is usually assumed to be important in western boundary currents,

but here is is seen to be two orders of magnitude smaller than the dominant terms.

The advection term, however, can be significant on the Equator. In the case here maximum value of $4.5 \ 10^{-4}$ is larger than the zonal pressure gradient. This term is also very sensitive to the vertical component of viscosity (κ). For a fixed wind stress and layer depth, the horizontal velocity components are proportional to κ^{-1}, but because the width of the upwelling region is itself proportional to $\kappa^{1/2}$, the maximum of $w\partial u/\partial z$ is proportional to $\kappa^{-5/2}$.

The figure also shows the force due to the horizontal component of the Coriolis vector. This is normally neglected in ocean models but in regions of strong upwelling it may have an effect. The results here show that at mid-depths on the Equator, the apparent force is larger than that due to horizontal viscosity but it is still much smaller than the dominant terms.

Figure A3 shows the corresponding terms for the meridional component of the momentum equation, positive values correspond to northward forces. The horizontal diffusion term is again very small.

The advection term shows minima and maxima close to Equator at the surface, at mid-depths and at the bottom of the layer. The mid-depth extreme are due to vertical advection, the top and bottom extrema due to horizontal advection in a region where the horizontal velocity is changing rapidly. The extreme values ($\pm 1.3 \ 10^{-4}$) are about a third of the zonal pressure gradient term, so although small they are not insignificant.

References

Bryden, H. L. and Brady, E. C.: Diagnostic Model of the Three-Dimensional Circulation in the Upper Equatorial Pacific Ocean, Journal of Physical Oceanography, 15, 1255–1273, 1985.

McCreary, J.: A Linear Stratified Ocean Model of the Equatorial Undercurrent, Phil.Trans.R.Soc.Lond.A., 298, 603–635, 1981.

Stommel, H.: Wind-drift near the Equator, Deep Sea Research, 6, 298–302, https://doi.org/10.1016/0146-6313(59)90088-7, 1960.